Waste products from the steel industry with NiO as additive as oxygen carrier for chemical-looping combustion

Magnus Rydén[1*], Erik Cleverstam[2], Anders Lyngfelt[1], Tobias Mattisson[1]

[1]Department of Energy and Environment
Chalmers University of Technology
SE-412 96, Göteborg, Sweden

[2]Department of Chemical and Biological Engineering
Chalmers University of Technology
S-412 96 Göteborg, Sweden

Abstract

Fe_2O_3-containing waste materials from the steel industry are proposed as oxygen carrier for chemical-looping combustion. Three such materials, red iron oxide, brown iron oxide and iron oxide scales, have been examined by oxidation and reduction experiments in a batch fluidized-bed reactor at temperatures between 800 and 950°C. NiO-based particles have been used as additive, in order to examine if it is possible to utilize the catalytic properties of metallic Ni to facilitate decomposition of hydrocarbons into more reactive combustion intermediates such as CO and H_2. The experiments indicated modest reactivity between the waste materials and CH_4, which was used as reducing gas. Adding small amounts of NiO-based particles to the sample increased the yield of CO_2 in a standard experiment, typically by a factor of 1.5-3.5. The fraction of unconverted fuel typically was reduced by 70-90%. The conversion of CH_4 to CO_2 was 94% at best, corresponding to a combustion efficiency of 96%. This was achieved using a bed mass corresponding to 57 kg oxygen carrier per MW fuel, of which only 5 wt% was NiO-based synthetic particles. The different materials fared differently well during the experiments. Red iron oxide was fairly stable, while brown iron oxide was soft and subject to considerable erosion. Iron oxide scales experienced increased reactivity and porosity as function of the numbers of reduction cycles.

Keywords: Chemical-Looping Combustion; Iron Oxide; Nickel Oxide

---

[*]*Corresponding author: Tel. (+46) 31 7721457, Email: magnus.ryden@chalmers.se*
International Journal of Greenhouse Gas Control 2009; 3: 693-703.

Abbreviations

CLC	Chemical-looping combustion
C_nH_m	Generic hydrocarbon fuel
F	Volumetric flow (L_n/min)
H_{lhw}	Lower heating value (J/mol)
L_n	Normal litres
m	Mass (g)
min	Minutes
Me	Generic oxygen carrier, reduced
MeO	Generic oxygen carrier, oxidized
n	Number of moles
nr	Number of reduction and oxidation cycles
P	Pressure (Pa)
p	Partial pressure (Pa)
R_0	Oxygen ratio, i.e. active oxygen content of oxygen carrier $(\%)$
t	Time (s, min)
v	Volume (L_n)
vol%	Percentage by volume
wt%	Percentage by weight
γ_{eff}	Combustion efficiency $(\%)$
γ_{red}	CO_2 yield $(\%)$
Φ_{CO}	CO fraction (%)
ω	Mass based degree of reduction (%)
χ	Reduction in unconverted fuel by addition of NiO (%)
σ	Provable synergy effect by addition of NiO (%)

Indexes

i	Generic index
max	Maximum
mo	Mixed oxide, oxide mixture
oc	Oxygen carrier
ox	Completely oxidized oxygen carrier
red	Completely reduced oxygen carrier
s	Sample of oxygen-carrier particles

1. Introduction

In later years, concerns that emissions of CO_2 from combustion of fossil fuels may lead to changes in the climate of the earth have been growing steadily. As a consequence, a majority of the scientific community now concludes that global CO_2 emissions would need to be reduced greatly in the future.

One way to reduce CO_2 emissions that is receiving increasing interest is carbon capture and storage, which involves capturing of CO_2 in emission sources and storing it where it is prevented from reaching the atmosphere. For example, CO_2 could be captured in flue gases from combustion or industrial processes, and stored in geological formations such as depleted oil fields or deep saline aquifers.

Chemical-looping combustion involves oxidation of a fuel using oxygen from a solid oxygen carrier. In this way the products are not diluted with N_2, and pure CO_2 for sequestration is obtained without the need for costly gas separation. Due to this favourable characteristic, chemical-looping combustion could have an important role to play in the global task to reduce anthropogenic CO_2 emissions.

2. Technical background

2.1 Chemical-looping combustion (CLC)

In chemical-looping combustion, two separate reactor vessels are used, one for air and one for fuel. A solid oxygen carrier performs the task of transporting oxygen between the reactors. Direct contact between fuel and air is avoided, so that the combustion products are not diluted with N_2, see Figure 1.

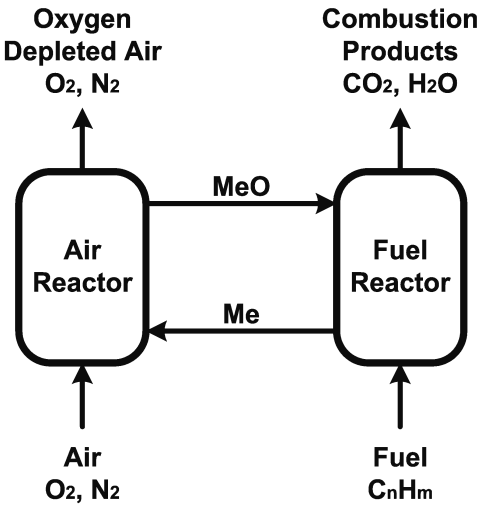

Figure 1. Schematic description of chemical-looping combustion.

Typically, the abbreviation MeO is used to describe the oxygen carrier in its oxidized form, while Me is used for the reduced form. This is because many potential oxygen-carrier materials are metal oxides.

The oxygen carrier circulates between the reactors. In the fuel reactor, it is reduced by the fuel, which in turn is oxidized to CO_2 and H_2O according to reaction (1). In the air reactor, it is oxidized to its initial state with O_2 from the combustion air according to reaction (2).

$$C_nH_m + (2n+½m)\ MeO \rightarrow n\ CO_2 + ½m\ H_2O + (2n+½m)\ Me \quad (1)$$

$$Me + ½\ O_2 \rightarrow MeO \quad (2)$$

The amount of energy released or required in each reactor vessel depends on the nature of the oxygen carrier and the fuel. Reaction (2) is always strongly exothermic. For most oxygen-carrier materials, reaction (1) is endothermic if the fuel is a hydrocarbon. Therefore the flow of solid oxygen carrier is also needed to transport sensible heat from the air reactor to the fuel reactor. The net energy released in the reactor system is the same as in ordinary combustion. This is apparent since combining reaction (1) and reaction (2) yields reaction (3), which is complete combustion of the fuel with O_2.

$$C_nH_m + (n+¼m)\ O_2 \rightarrow n\ CO_2 + ½m\ H_2O \quad (3)$$

Compared to conventional combustion, chemical-looping combustion has several potential benefits. The exhaust gas from the air reactor is harmless, consisting mainly of N_2 and possibly some O_2. There is no thermal formation of NO_X since regeneration of the oxygen carrier takes place without flame and at moderate temperatures. The gas from the fuel reactor consists of CO_2 and H_2O, so cooling in a condenser is all that is needed to obtain almost pure CO_2.

Chemical-looping combustion could replace ordinary combustion in many common large-scale applications. The main advantage would be more or less complete CO_2 capture, without necessarily decreasing the overall process efficiency. This is a rare feature among technologies proposed for CO_2 capture, which typically comes with considerable costs and energy penalties. Therefore, chemical-looping combustion is a very attractive technology for power generation with CO_2 capture of fossil fuels such as coal or natural gas. Naturally, it could also be used for other large scale applications, for example combustion of waste products such as refinery gas, or for generation of heat to industrial processes or district heating systems. Another interesting option could be to use chemical-looping combustion as heat source for production of H_2 via the endothermic steam reforming reaction. This way it would be possible to produce H_2 from fossil

fuels such as natural gas without CO_2 emissions to the atmosphere. Obtained H_2 could be used as emission free fuel for vehicles and other applications.

In practice, a chemical-looping combustion process could be designed in different ways, but circulating fluidized beds with oxygen-carrier particles used as bed material are likely to have an advantage over other alternatives since this design is well established, straightforward, provides good contact between gas and solids and allows a smooth flow of oxygen-carrier particles between the reactors.

2.2 Oxygen-carrier materials

A feasible oxygen-carrier material for chemical-looping combustion should:

- Have high reactivity with fuel and oxygen.
- Be thermodynamically capable to convert a large share of the fuel to CO_2 and H_2O.
- Have a sufficiently high oxygen ratio, e.g. the mass fraction of the material that is oxygen which can react according to reaction (1) should be decently high.
- Have low tendency for fragmentation, attrition, agglomeration and other kinds of mechanical or thermal degeneration.
- Not promote extensive formation of solid carbon in the fuel reactor.
- Preferably be cheap and environmentally sound.

Metal oxides such as NiO, Fe_2O_3, Mn_3O_4 and CuO supported on inert carrier material such as Al_2O_3 or stabilized ZrO_2 are likely candidates to meet those criteria. An overview of the research dealing with these kinds of oxygen-carriers can be found in the works of Cho (2005), Johansson, M. (2007) and Adánez et al. (2003a). Information about other potential oxygen-carrier materials can be found in the work of Jerndal et al. (2006), which includes a theoretical examination of 27 different oxide systems. Carbon formation on oxygen-carrier particles for chemical-looping combustion has been specifically examined by Cho et al. (2005b). Continuous chemical-looping combustion in circulating fluidized beds has been demonstrated by Lyngfelt et al. (2004), Ryu et al. (2004), Johansson, E. (2006a, 2006b), Abad et al. (2006, 2007a), Adánez et al. (2003b), Linderholm et al. (2008, 2009a, 2009b), De Diego et al. (2007), Berguerand and Lyngfelt (2008a, 2008b), Rydén et al. (2008b), Kolbitsch et al. (2008) and Pröll et all. (2008). Reaction kinetics for oxygen carriers have been examined by Abad et al. (2007b, 2007c) and Zafar et al. (2007a, 2007b). The effects of pressure on the behaviour of oxygen-carrier materials have been examined by García-Labiano et al. (2006).

An overview of various subjects regarding chemical-looping combustion, such as design of experimental reactors, power production with CO_2 capture, use of solid fuels, chemical looping for production of H_2 and synthesis gas, and more about oxygen-carriers can be found in the doctoral theses by Brandvoll (2005), Johansson, E (2005), Wolf (2004), Kronberger (2005), Naqvi (2006), Leion (2008a) and Rydén (2008a).

2.3 Minerals, ores and waste products as oxygen carrier

Naturally, manufacture of synthetic oxygen-carrier particles is associated with some costs. Therefore, it has been suggested that it could be feasible to use cheap and abundant materials such as natural minerals and ores or waste products from the industry as oxygen carrier instead. This would be cheaper, especially if the oxygen carrier has limited life time, which could be the case for some applications.

The most well examined such material is the naturally occurring mineral ilmenite, $FeTiO_3$, which has been examined by Berguerand and Lyngfelt (2008a, 2008b), Leion et al. (2008b, 2009a), Kolbitsch et al (2008) and Pröll et al (2008). Further, Leion et al. (2008a, 2009a, 2009b) have also examined various iron and manganese ores, including industrial waste products prepared in the same way as those examined in this paper.

2.4 Mixed oxides as oxygen carrier

A mixed-oxide oxygen carrier for chemical-looping combustion consists of more than one active phase, and should be able to take advantage of favourable characteristics of each, i.e. create some kind of positive synergy effect. Such materials could be produced in different ways, for example by mixing different metal oxides particles in a fluidized bed, by impregnating a second active phase onto existing particles, or by producing materials with multiple active phases directly in the manufacturing process.

There are many synergy effects that could possibly be achieved. Jin et al. (1998) prepared a CoO-NiO particle on yttria-stabilized zirconia, which reportedly suppressed formation of solid carbon on the particle surface. Son and Kim (2006) applied NiO and Fe_2O_3 in different ratios onto bentonite, using NiO to provide high reactivity and Fe_2O_3 to improve the particle strength. Adánez et al. (2006) added CuO to a NiO-based oxygen carrier in order to improve the conversion of CO and H_2, which is thermodynamically constrained on NiO.

In this study, another approach is used. When reduced by a fuel, NiO is converted directly to metallic Ni, which is well known to catalyse decomposition of CH_4 and other hydrocarbons. Mattisson et al. (2008) found that almost complete conversion of CH_4 into combustion products can be achieved with a very small bed of NiO material, and that the reaction proceeds with CO

and H_2 as intermediates. Unfortunately, using NiO as oxygen carrier for chemical-looping combustion has some drawbacks. NiO is comparably expensive and also a health hazard. Further, the conversion of hydrocarbons into H_2O and CO_2 at relevant temperatures is limited to slightly above 99% due to thermodynamical constraints. In contrast, Fe_2O_3 is cheap, abundant, non toxic and can convert hydrocarbon fuel completely into CO_2 and H_2O. The reactivity with CH_4 is low compared to NiO. However, the reactivity of Fe_2O_3 with CO and H_2 has been found to be high, see Mattission et al. (2006). Therefore it seems reasonable to believe that the rate-limiting step for chemical-looping combustion of hydrocarbons using Fe_2O_3 as oxygen carrier is conversion of CH_4 into reactive intermediates such as CO and H_2, see Johansson, M et al. (2004). Based on these characteristics, a mixed-oxide oxygen carrier that consists of small amounts of NiO as catalyst and Fe_2O_3 as the main oxygen carrier could have advantages compared to the alternatives. Small amounts of NiO would likely be sufficient to facilitate decomposition of hydrocarbons and CH_4 into CO and H_2, which reacts fast with Fe_2O_3. In a study by Johansson, M et al.(2004), it was found that addition of as little as 1 wt% NiO-based particles to a sample of Fe_2O_3 improved the capacity of the sample to convert CH_4 into CO_2 and H_2O considerably. If feasible, such oxide mixtures would reduce the cost for of premium oxygen carriers considerably. The potential impact on the environment and human health would be significantly reduced compared to NiO based oxygen carriers, but would still be present to some extent. Therefore any process involving this type of oxygen carriers would require strict regulation and monitoring.

2.5 The aim of this study

The objective of this study is to examine waste materials from the steel industry consisting mainly of Fe_2O_3 as oxygen-carrier material for chemical-looping combustion, and also to examine if it is possible to improve the reactivity of such materials by addition of small amounts of catalytic NiO-based material.

3. Experimental

3.1 Oxygen-carrier materials

Three different waste products from the steel industry have been examined, namely red iron oxide, brown iron oxide and iron oxide scales. All three materials are considered to have no or very little economic value. They were provided by SSAB, a major steel manufacturing company.

Red iron oxide is a waste product from steel sheet production. It was obtained as a fine powder which was freeze granulated into particles, sintered at 950°C and sieved to a size range of 125-

180 μm. Elemental analysis showed that the resulting particles consisted of over 99 wt% Fe_2O_3, with traces of Si, Mn, Al and P, presumably present mainly as oxides.

Brown iron oxide is a waste product produced during surface refinement of steel sheeting. It was obtained as a fine powder which was freeze granulated into particles, sintered at 1100°C and sieved into a size range of 125-180 μm. Analysis showed that the resulting particles consisted of about 99 wt% Fe_2O_3, with Si, Mn, Al, Ca, P, Ti and oxides of these impurities making up the difference.

Iron oxide scales is produced during rolling of steel sheets. In order to be useful for chemical-looping applications, the oxide scales were heat treated at 950°C for 24 hours, in order to remove residual oils. The resulting product consisted of over 99 wt% Fe_2O_3, with Si, Mn, Al, Ca, P and oxides of these impurities making up the balance. The dry oxide scales were crushed, ground and sieved into a suitable size range, i.e. 125-180 μm.

Two different NiO materials were used as additives. N6AM1400 is a synthetic particle that consists of 60 wt% NiO supported on $MgAl_2O_4$, and was produced from fine chemical powders by freeze granulation and sintering for 6 hours at 1400ºC. Ni-olivine is olivine sand, $(Fe,Mg)_2SiO_4$, which has been impregnated with small amounts of NiO, in order to be used for cracking tars during gasification of biomass.

By itself, olivine does not react with CH_4 at the used condition, and since it contains only about 1 wt% NiO its oxygen-carrier capacity should be neglectable for the experiments conducted in this paper. Ni-olivine has been tested in order to examine if it could be useful for cracking CH_4 during chemical looping combustion. A summary of used oxygen carrier materials can be found in Table 1.

Table 1. *Summary of oxygen carrier materials.*

Oxygen carrier	**Density (kg/m^3)**	**Porosity**	**Crushing strength (N)**
Iron oxide scales	4013	0.21	8.3
Red iron oxide	2117	0.59	0.8
Brown iron oxide	2241	0.56	0.6
N6AM1400	3002	0.42	2.2
Ni-olivine	2339	0.31	4.5

The reason why freeze granulation was used for production of the examined oxygen carriers is that this method is suitable for production of small batches of particles. However, this manufacturing method would not be economically feasible in larger scale. Therefore, spray drying would seem like a better choice for industrial scale applications. Spray drying is a very cheap

method to produce large batches of particles, and can be used to produce particles with similar properties as freeze granulations.

In table 1, the density is the calculated directly by weighing a certain volume of particles, and dividing with a packing factor. The porosity is a comparison of this calculated density to the density of solid material of with the same composition as the oxygen carrier. Therefore, these numbers are comparably rough estimations. Basically, a high number indicates that the particle is highly porous. Crushing strength reflects the average force that is needed to crush a particles in the size span 180-250 μm. Scanning electron microscope pictures of the oxide materials can be found in Figure 2.

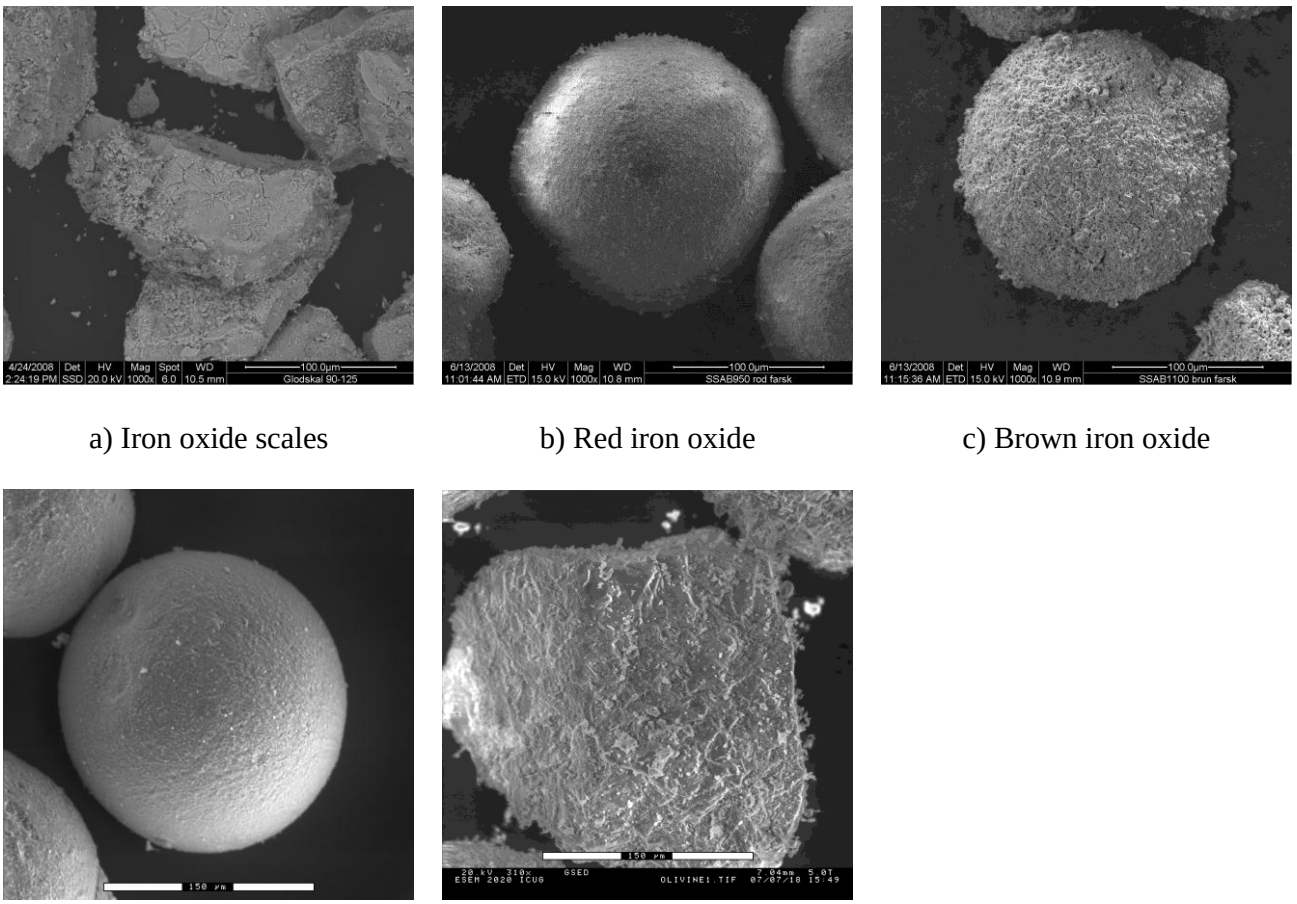

a) Iron oxide scales b) Red iron oxide c) Brown iron oxide

d) N6AM1400 e) Ni-olivine

Figure 2. Pictures of fresh 100-150 μm oxygen-carrier particles.

In Table 1 and Figure 2 it can be seen that there is a large difference in density, porosity and geometry between the oxygen carriers used. Iron oxide scales and olivine sand are hard, less porous and non-spherical, while freeze-granulated particles are spherical, porous and comparably soft.

When used as oxygen carrier, iron oxide can be reduced in several steps. For chemical-looping combustion, only the first step, reduction of Fe_2O_3 to Fe_3O_4, is of interest. Further reduction to FeO and metallic Fe should be avoided, since formation of FeO could result in fluidization problems, and also in poor conversion of the fuel due to less favourable thermodynamics. By contrast, NiO is reduced directly to metallic Ni, and can not be reduced further. A summary of the expected reduction reactions can be found in Table 3, in section 3.3 below.

3.2 Reactivity tests in batch fluidized-bed reactor

The experiments were conducted in an 820 mm long quartz reactor with an inner diameter of 22 mm. A porous quartz plate, on which the oxygen-carrier sample is applied, is located 370 mm above the bottom. During operation, the sample is fluidized by adding gas to the bottom of the reactor, and the porous plate acts as gas distributor. In order to reach suitable temperature the reactor is placed inside an electrically heated furnace. Reactor temperature is measured below and above the porous plate, using thermocouples enclosed in quartz shells. The pressure drop over the bed is measured with pressure transducers. The gas from the reactor is led to a cooler, in which the water is removed. Following this step the volumetric flow of gas is measured, and the composition analyzed. The concentrations of CO_2, CO and CH_4 are measured using infrared analyzers, while O_2 is measured with paramagnetic sensors.

The aim of the batch experiment was to examine the oxidation and reduction behaviour of the oxygen carrier, and to examine if the reactivity could be improved by adding NiO. In order to do so, a sample of 12.6-15 g particles was applied to the porous plate. Then the reactor was heated to the desired temperature, which for these experiments was 800-950°C. During this period the reactor was fluidized with inert N_2. Chemical-looping combustion was simulated by alternating between reducing and oxidizing conditions. Firstly, the sample was reduced with 0.36-0.45 L_n/min CH_4 for 20-30 seconds. This corresponds to 57 kg oxygen carrier per MW fuel. Following the reduction period, the sample was reoxidized with 1.0 L_n/min of a gas mix consisting of 5 vol% O_2 and 95 vol% N_2. The reason for not using air is that reaction (2) is highly exothermic, so a low concentration of O_2 is used in order to avoid extensive heating of the reactor. After the oxidation period, the sample was ready to be reduced again and so on. To avoid oxygen and methane mixing during the shifts between reduction and oxidation, 0.45 L_n/min N_2 was introduced during 180 s after each reduction and each oxidation period. A summary of experiments conducted can be found in Table 2.

Table 2. *Summary of experiments performed.*

Base oxide	Additive	CH_4 flow (L_n/min)	T (°C)	Reductions (nr)
15 g red iron oxide		0.45	950	17
15 g red iron oxide		0.45	800-950	17
14.25 g red iron oxide	0.75 g N6AM1400	0.45	950	12
14.25 g red iron oxide	0.75 g N6AM1400	0.45	850-950	11
14.25 g red iron oxide	0.75 g Ni-olivine	0.45	850-950	17
13.6 g brown iron oxide		0.41	850-950	11
12 g brown iron oxide	0.6 g N6AM1400	0.36	850-950	13
15 g iron oxide scales		0.45	950	19
15 g iron oxide scales		0.45	850-950	19
14.25 g iron oxide scales	0.75 g N6AM1400	0.45	850-950	11

3.3 Evaluation of data

The oxygen ratio, R_0, is defined in expression (4), and the degree of oxidation of the oxygen carrier, X, is defined in expression (5).

$$R_0 = (m_{s,ox} - m_{s,red}) / m_{s,ox} \tag{4}$$

$$X = \frac{m_s - m_{s,red}}{m_{s,ox} - m_{s,red}} \tag{5}$$

In expressions (4-5), m_s is the actual mass of sample, $m_{s,ox}$ is the mass of the sample when fully oxidized, and $m_{s,red}$ the mass of the sample while completely reduced. R_0 describes the mass fraction of the particle that can theoretically be released as oxygen during operation. X describes the oxygen content of a sample relative to the theoretical maximum R_0. X can be calculated as function of time using expression (6).

$$X_i = X_{i-1} - \int_{t_o}^{t_1} \frac{n_{out,tot}}{n_{o,oc} \times P_{tot}} \times (4p_{CO_2,fr} + 3p_{CO,fr} - p_{H_2,fr})dt \tag{6}$$

In expression (6), X_i is the conversion as a function of time for period i, X_{i-1} is the conversion after the preceding period, t_0 and t_1 are the times for the start and finish of the period respectively, $n_{o,oc}$ is the moles of active oxygen in the unreacted oxygen carrier, $n_{out,tot}$ is the molar flow of the gas leaving the reactor after the water has been removed, P_{tot} is the total pressure, and $p_{CO2,fr}$, $p_{CO,fr}$ and $p_{H2,fr}$ are the outlet partial pressures of CO_2, H_2 and CO after the removal of H_2O. $p_{H2,fr}$ was not measured online but assumed to be related to the outlet partial pressure of CO and CO_2 through an empirical relation based on the equilibrium of the gas-shift reaction.

In this paper, the mass based degree of reduction, ω, is used to describe the reduction of the oxygen carrier particles. ω describes how much oxygen that has been removed from the oxygen carrier compared to its oxidized weight, and is defined in expression (7).

$$\omega = \frac{m_s}{m_{s,ox}} = 1 + R_o(X - 1) \tag{7}$$

The mass conversion ω for various reduction steps can be found in Table 3, in which it has been assumed that the main oxygen carrier consists of Fe_2O_3, and that reduction of NiO to Ni is fast and takes place prior to reduction of Fe_2O_3 to Fe_3O_4,.

Table 3. *Expected ω for various reactions and oxygen carriers.*

Reaction	ω_{Fe2O3}	$\omega_{N6AM1400}$	$\omega_{95/5\ Fe2O3/N6AM1400}$
$NiO \rightarrow Ni + ½O_2$	-	1.000 - 0.872	1.000 - 0.994
$3Fe_2O_3 \rightarrow 2Fe_3O_4 + ½O_2$	1.000 - 0.967	-	0.994 - 0.962
$Fe_3O_4 \rightarrow 3FeO + ½O_2$	0.967 - 0.900	-	0.962 - 0.898
$FeO \rightarrow Fe + ½O_2$	0.900 - 0.699	-	0.898 - 0.708

In table 3, it can be seen that ω below 0.967 should be avoided for experiments without addition of N6AM1400, while the corresponding number for experiments with addition of N6AM1400 is 0.962. Below these numbers formation of FeO could be expected, which could result in defluidization of the sample and in poor conversion of the fuel due to less favourable thermodynamic conditions. It should be mentioned that the Ni-olivine only contains about 1 wt% Ni, which means that these particles can only contribute an insignificant amount of oxygen during the reduction.

The CO_2 yield, γ_{red}, is defined in expression (8), and the corresponding CO fraction, Φ_{CO}, is defined in expression (9). Under ideal circumstances, γ_{red} should be 1 while Φ_{CO} should be 0.

$$\gamma_{red} = p_{CO2,out} / (p_{CH4,out} + p_{CO2,out} + p_{CO,out}) \tag{8}$$

$$\Phi_{CO} = p_{CO,out} / (p_{CH4,out} + p_{CO2,out} + p_{CO,out}) \tag{9}$$

The performance of a chemical-looping combustion process can also be expressed with the combustion efficiency, γ_{eff}, which is defined in expression [11].

$$\gamma_{eff} = 1 - \frac{n_{CH4,fr} \times H_{lhw,CH4} + n_{CO,fr} \times H_{lhw,CO} + n_{H2,fr} \times H_{lhw,H2}}{n_{fuel,in} \times H_{lhw,fuel}} \quad (10)$$

In expression (10), n_i is the molar flows of each component, while $H_{lhw,i}$ is its lower heating value. The definition does not take into account the possibility of formation of solid carbon in the fuel reactor or that higher hydrocarbons could be present in the fuel-reactor gas. Neither of these phenomena is believed to have occurred at any significant degree during the experiments presented in this paper.

4. Results

4.1 Reduction experiments with CH_4

By themselves, the waste materials showed modest reactivity with CH_4. Resulting gas composition during reduction at 950°C can be found in Figure 3.

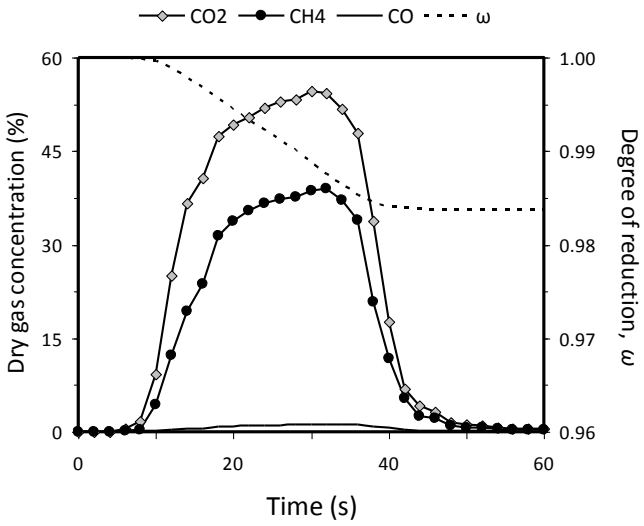

Figure 3a) Reduction of 15 g red iron oxide with 0.45 L_n/min CH_4 at 950°C, 4th reduction cycle.

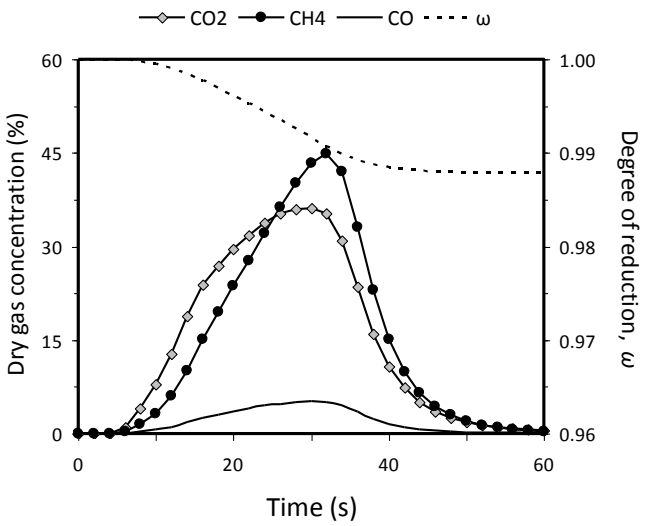

Figure 3b) Reduction of 13.6 g brown iron oxide with 0.41 L_n/min CH_4 at 950°C, 4th reduction cycle.

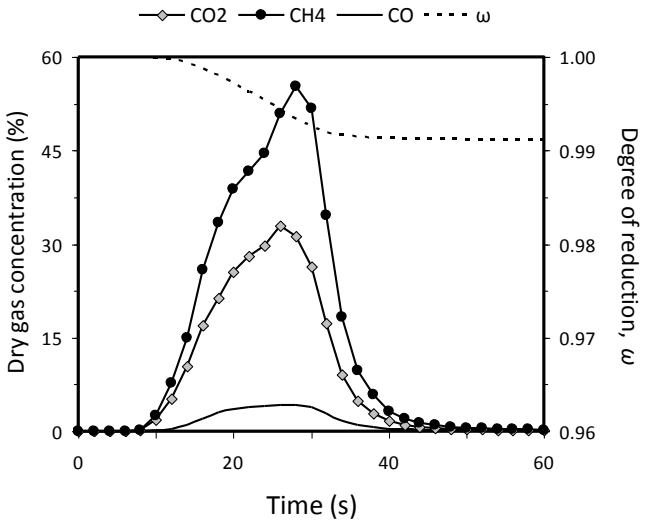

Figure 3c) Reduction of 15 g iron oxide scales with 0.45 L_n/min CH_4 at 950°C. 18th reduction cycle.

In Figure 3, it can be seen that the red and brown iron oxide reacted slightly faster and therefore produced a higher CO_2 peak compared to iron oxide scales. y_{red} was ≈70% for red and brown iron oxide in the very beginning of the reduction period. Iron oxide scales increased in reactivity as function of reduction cycle, as will be discussed in section 4.4 below. For the 18th reduction shown in Figure 3c, y_{red} was ≈40% in the very beginning of the reduction period. The reason for the higher reactivity of the freeze granulated particles is likely that they are more porous and thus have larger active surface than iron oxide scales.

In Figure 3, it can also be seen that red iron oxide showed considerably more favourable reduction behaviour than brown iron oxide, with higher concentration of CO_2 sustained for a longer period of time. Further, Φ_{CO} was ≈5% for brown iron oxide during most of the reduction period, but only ≈1% for red iron oxide. Particles of red and brown iron oxide hadhave similar physical properties, so there are no obvious reason for the difference in reactivity, except that brown iron oxide contained traces of Ca and Ti, in addition to impurities also present in red iron oxide. As comparison, Φ_{CO} was 3-6% in the 18th reduction for iron oxide scales. Here CO was low in the beginning of the reduction period but increased with time.

Gas composition during reduction of samples with 5 wt% addition of the NiO based N6AM1400 particles at 950°C can be found in Figure 4.

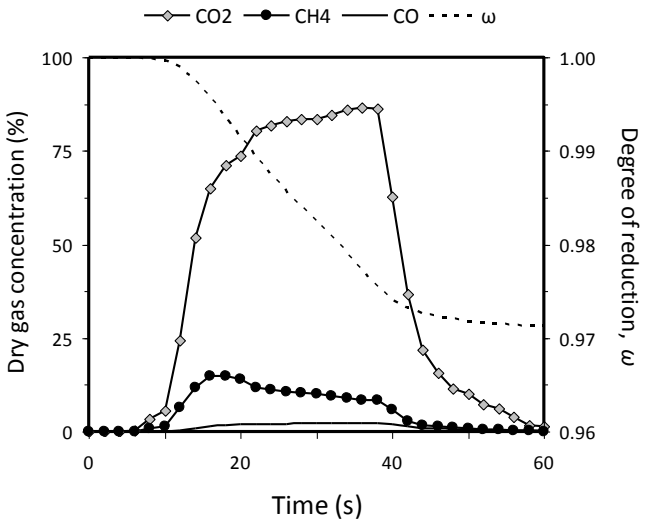

Figure 4a) Reduction of 14.25 g red iron oxide and 0.75 g N6AM1400 with 0.45 L_n/min CH_4 at 950°C, 4th reduction cycle.

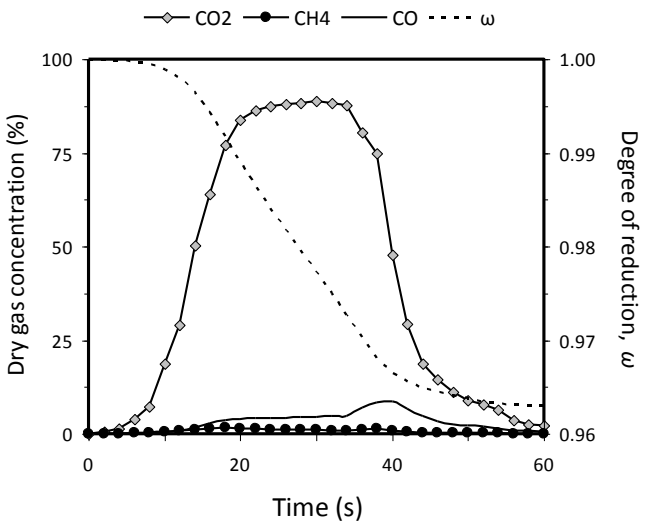

Figure 4b) Reduction of 12g brown iron oxide and 0.6 g N6AM1400 with 0.36 L_n/min CH_4 at 950°C, 4th reduction cycle.

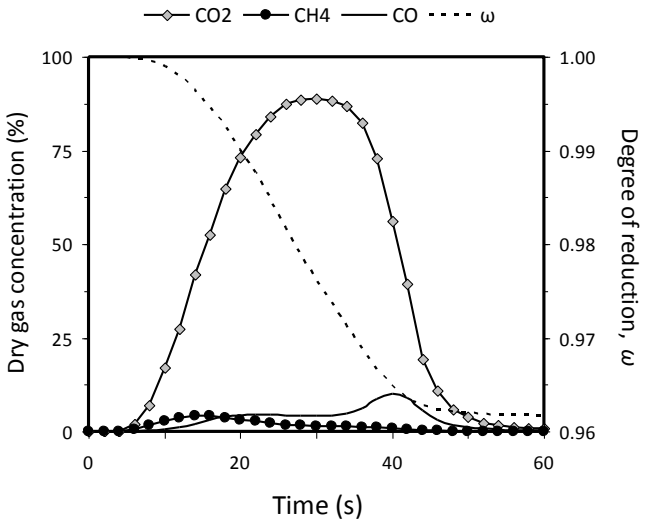

Figure 4c) Reduction of 14.25 g iron oxide scales and 0.75 g N6AM1400 with 0.45 L_n/min CH_4 at 950°C. 4th reduction cycle.

In Figure 4, it can be seen that CO_2 concentrations in the range of 90 vol% was obtained for all three oxygen carriers, which is a large improvement compared to samples without addition of NiO. y_{red} was at most ≈94% for brown iron oxide and iron oxide scales, and ≈90% for red iron oxide. This corresponds to combustion efficiencies of up to 96%.

The pattern from the experiments conducted without NiO, that red iron oxide produced less CO than brown iron oxide, was valid for experiments with NiO addition as well. Φ_{CO} was ≈3-6% for brown iron oxide and iron oxide scales, but only 1-2% for red iron oxide. The fraction of unconverted CH_4 was considerably higher for red iron oxides though.

The improvement in reactivity for iron oxide scales and brown iron oxide was larger compared to red iron oxide. So large in fact, that these particles risked becoming reduced too far during the experiments. The small bump in the concentration of CO experienced at t≈40 s for brown iron oxide and iron oxide scales could be an indication that formation of FeO has been initiated, which should occur no later than when ω is ≈0.962, according to Table 3. Reduction of Fe_3O_4 to FeO should result in increased CO concentration because of thermodynamic constraints.

In Figure 5, the CO_2 yield has been plotted as function of the mass-based degree of reduction for reduction of red iron oxide at temperatures between 850-950°C, with and without addition of N6AM1400.

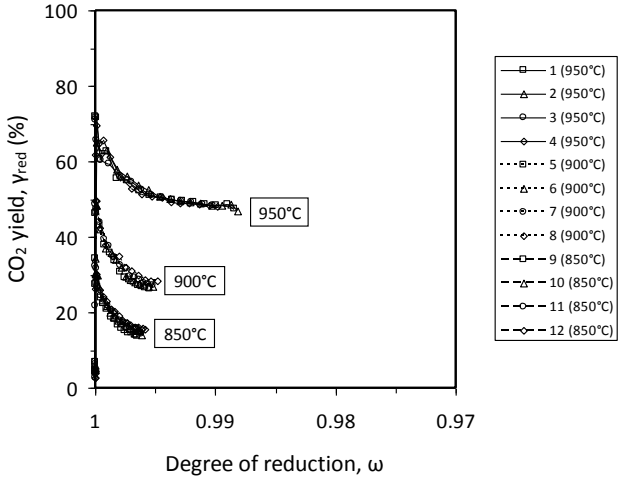

Figure 5a) γ_{red} as function of ω for red iron oxide for different reduction cycles and temperatures.

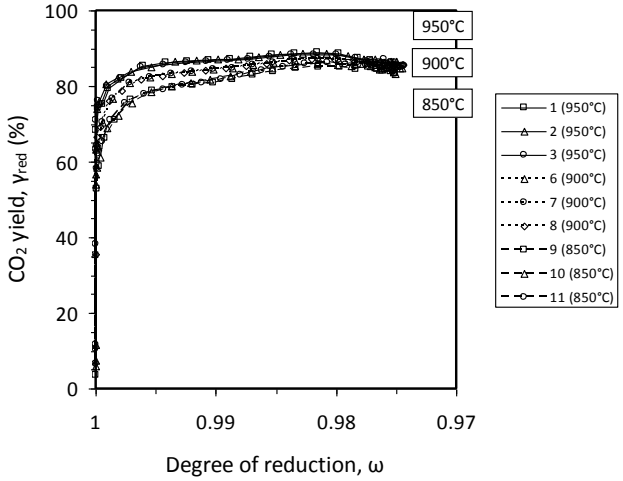

Figure 5b) γ_{red} as function of ω for red iron oxide with 5 wt% N6AM1400 for different reduction cycles and temperatures.

In Figure 5a, it can be seen that reduced reactor temperature resulted in reduced rate of reaction, i.e. the CO_2 yield is higher and the sample becomes reduced to lower ω. This could be expected, since chemical reaction in general proceeds faster at high temperatures. In Figure 5b, it can be seen that the CO_2 yield is much larger for experiments when N6AM1400 has been added to the sample, and that the effect of reduced temperature was much smaller here.

In Figures 3-5, it can be seen that the reduction evolves differently depending on whether N6AM1400 was added to the sample. Without addition of N6AM1400, γ_{red} is highest in the beginning of the reduction period, when ω is high. When oxygen is removed from the sample and ω decreases, γ_{red} decreases as well. Addition of N6AM1400 reverses this pattern. Here γ_{red} is comparable to experiments without addition of N6AM1400 when ω is close to 1, but as soon as

the particles are reduced somewhat and metallic Ni is obtained, γ_{red} starts to increase. This behaviour supports the theory that metallic Ni helps decomposing CH_4 into compounds more reactive with Fe_2O_3.

Adding 5 wt% Ni-olivine to red iron oxide particles resulted in a moderate increase in the CO_2 yield, see Figure 6.

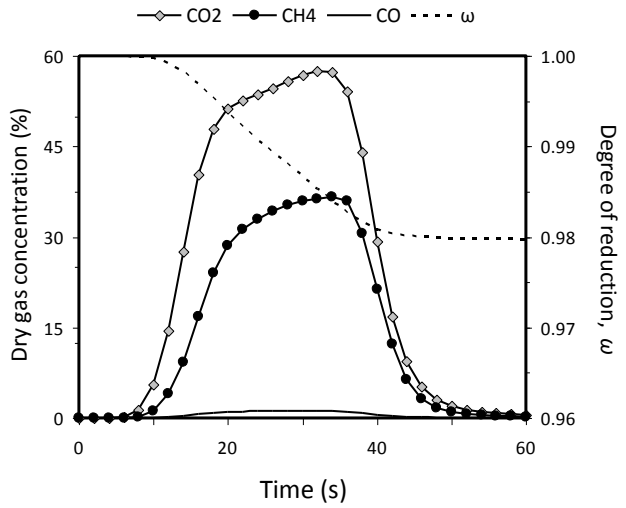

Fig 6a) Reduction of 14.25 g red iron oxide and 0.75 g Ni-olivine with 0.45 L_n/min CH_4 at 950°C, 4th reduction cycle.

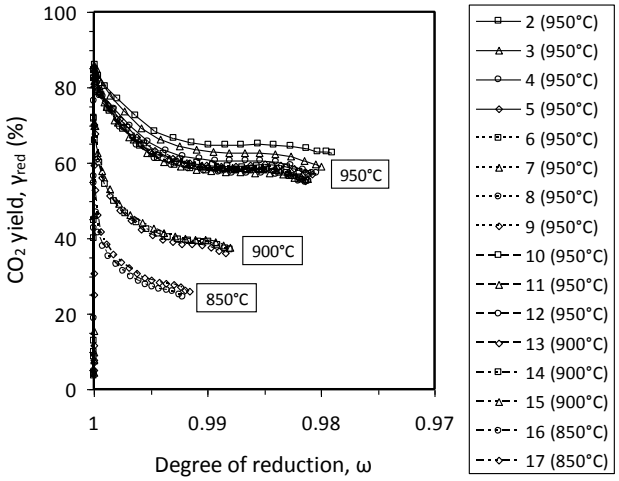

Figure 6b) γ_{red} as function of ω for red iron oxide with 5 wt% Ni-olivine for different reduction cycles and temperatures.

In many aspects, the reduction shown in Figure 6 is similar to the corresponding reduction without Ni-olivine, i.e. Figure 3a and Figure 5a respectively. However, the CO_2 concentration is slightly higher, the CH_4 concentration is slightly lower, and a lower ω is achieved for each reduction cycle. The improvement in CO_2 yield is 5-10% at 950°C, and considerably larger at lower temperatures.

Brown iron oxide without addition of N6AM1400 behaved similarly to red iron oxide with respect to temperature dependence, i.e. Figure 5a illustrates these experiments perfectly well. With addition of 5 wt% N6AM1400, brown iron oxide provided slightly higher CO_2 yield than red iron oxide at 950ºC, but slightly lower at 850°C.

The interpretation of results obtained with iron oxide scales at different temperatures is uncertain, since the reactivity of these particles improved with each reduction cycle, as will be further explained in section 4.4 below. In general, iron oxide scales appears to have been less sensitive for reduced temperature compared to red iron oxide though.

4.2 Effect of N6AM1400 and Ni-olivine addition

In table 4, some performance data derived from reductions such as those shown in Figures 3-6 are shown, for two different temperatures.

Table 4. *Example of performance data for examined mixed-oxide systems, * indicate experiments with Ni-olivine rather than N6AM1400.*

	T_{fr} (°C)	$\gamma_{eff,max}$ (%)	$\gamma_{eff,max,mo}$ (%)	$v_{CO2,30s}$ (L_n)	$v_{CO2,30s,mo}$ (L_n)	χ (%)	σ (%)
SSAB Red	950	73.1	92.1	0.085	0.156	71	43
SSAB Red	850	41.4	88.3	0.020	0.105	80	254
SSAB Brown	950	73.7	96.3	0.045	0.153	86	164
SSAB Brown	850	34.8	83.1	0.011	0.075	74	271
Iron Oxide Scales	950	50.5	95.8	0.029	0.143	92	275
Iron Oxide Scales	850	47.1	89.9	0.027	0.129	81	251
SSAB Red*	950	73.1	81.8*	0.085	0.093*	32*	9*
SSAB Red*	850	41.4	51.3*	0.020	0.036*	17*	77*

In Table 4, $\gamma_{eff,max}$ is the highest combustion efficiency measured during reduction of the base oxide, following the initial seconds when the products are slightly diluted with N_2 due to imperfect plug flow. $\gamma_{eff,max,mo}$ is the corresponding peak value for the case with 5 wt% N6AM1400 addition. $v_{CO2,30s}$ and $v_{CO2,30s,mo}$ are the volumes of CO_2 produced during 30 s of reduction expressed in normal litres.

The improvement resulting from addition of catalytic material is expressed in two ways. χ describes the reduction in unconverted fuel passing through the reactor when the reactivity is at its highest, and is defined in expression (11).

$$\chi = 100 \times (\gamma_{eff,max,mo} - \gamma_{eff,max}) / (100 - \gamma_{eff,max}) \quad (11)$$

However, improved conversion of the fuel is insufficient proof that there is an actual synergy effect of mixing NiO and Fe_2O_3 as discussed in the introduction, i.e. that metallic Ni converts CH_4 to CO and H_2, which subsequently reacts with Fe_2O_3. This is because Ni-based materials have higher reactivity and oxygen transfer capacity than the Fe_2O_3-based materials. Therefore it could be expected that the addition of such a material should result in increased fuel conversion, even if there is no synergy effect. One way of demonstrating that there really is a synergistic effect is to show that there is an improvement in reactivity, even after subtracting the possible direct contribution of added NiO. This was done by calculating the increase in CO_2 production over a certain reduction period, σ, which is defined in expression (12).

$$\sigma = 100 \times [\ (v_{CO2,30s,mo} - v_{CO2,NiO}) / v_{CO2,30s} - 1\ ] \quad (12)$$

σ describes the increase in the total amount of CO_2 produced during 30 s, that is achieved by addition of 5 wt% NiO material. In expression (12), $v_{CO2,NiO}$ reflects the contribution of oxygen carrier capacity brought by the NiO addition, if it is assumed that added NiO is reduced to Ni by the fuel and that the products of this process are only CO_2 and H_2O. If the fuel is CH_4, $v_{CO2,NiO}$ is 0.0342 L_n for 0.75 g N6AM1400 and ≈0.0006 L_n for 0.75 g Ni-olivine.

In Table 4, it can be seen that adding 5 wt% N6AM1400 clearly has a positive effect on fuel conversion. The fraction of unconverted fuel was reduced with 71-92%, which is a large improvement. As for the provable synergy effect σ, most often 2.5-3.8 times more CO_2 was produced with NiO addition. So it can safely be concluded that there is a synergy effect of adding NiO to a sample of Fe_2O_3, i.e. obtained Ni catalyses decomposition to CO and H_2, which reacts further with Fe_2O_3 to CO_2 and H_2O. The effect is substantial and definitely interesting for practical chemical-looping combustion applications.

The improvement obtained with SSAB Red at 950°C was smaller compared to other experiments. However, this likely was an effect of the chosen experimental conditions. At 950°C, the mentioned oxygen carrier already provided decently high fuel conversion, without addition of NiO. Therefore, the possible improvements were in the same order of magnitude as the extra oxygen carrier capacity provided by the NiO-particles, and the apparent synergy could not reach as high values as for less reactive oxygen carriers.

In Table 4, it can also be seen that addition of Ni-olivine resulted in some improvements. The combustion efficiency increased and slightly more CO_2 was produced during a typical reduction period. This shows that even very small amounts of NiO-addition have a positive effect on the fuel conversion. For these experiments, the NiO content of the particle bed should have been less than 0.05 wt%.

4.3 Oxidation of reduced particles

Reoxidation of reduced particles was an undramatic process. Basically, the oxidation reaction was sufficiency fast for all added O_2 to react with the particles, until they were completely reoxidized. No CO_2 or CO was formed during reoxidation, so there was no carbon deposition during the reduction period.

4.4 Stability of examined oxygen-carrier particles

Used samples have been examined by x-ray powder diffraction, but it was not possible to verify any unexpected phases in any of the materials. Used particles have also been examined by scanning electron microscopy. Pictures of used particles can be found in Figure 7.

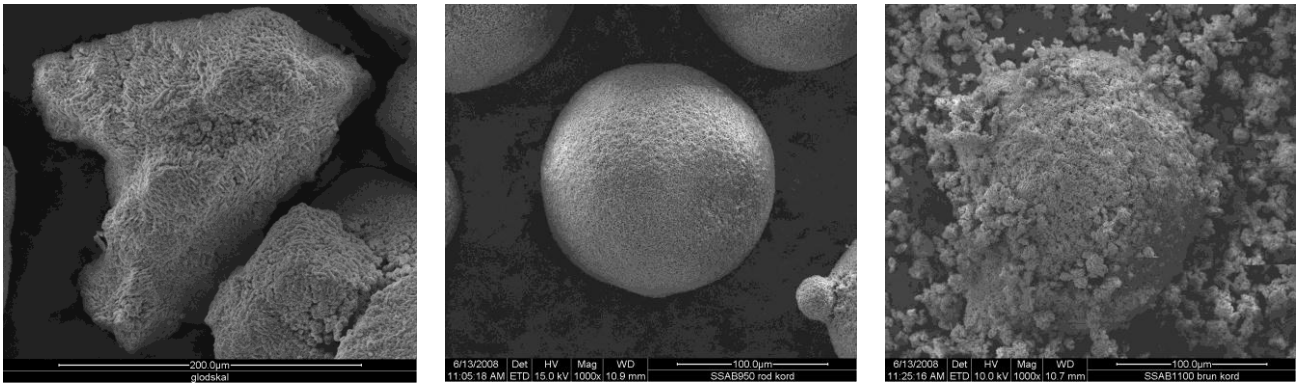

a) Iron oxide scales *b) Red iron oxide* *c) Brown iron oxide*

Figure 7. Pictures of used 100-200 µm oxygen-carrier particles.

Red iron oxide fluidized well and provided the best and most reliable results of the examined materials. After a few initial reductions with slightly higher conversion of CH_4, the particles stabilized and provided very predictable results, as is demonstrated in Figure 5 above. Red iron oxide also retained its physical properties such as density and porosity well during the course of the experiments. Comparison between Figure 2b and Figure 7b verifies that used particles retained their physiology well.

Particles of brown iron oxide fluidized decently, but were soft and experienced considerable erosion. In Figure 7c, it can be seen clearly that the particles have started to break apart, forming fines. During a reduction series of 11-13 cycles, roughly 10% of added material was lost due to elutriation of fines. The sample to which N6AM1400 had been added also experienced a considerable reduction in density, which makes the interpretation of these results somewhat uncertain.

In early experiments, iron oxide scales defluidized during the inert phase. This is not surprising, since iron oxide scales had higher density and lower sphericity than the freeze granulated particles. Increasing the inert flow to 0.60 L_n/min more or less solved this problem. Such defluidization seems unlikely to become a problem in a real-world reactor, where much higher gas velocities would be used compared to the experiments presented in this study. The superficial gas velocity was in the order of 0.1 m/s in the experiments performed in this study, while a real-world process would utilize velocities at least an order of magnitude greater.

Further, iron oxide scales did not provide entirely stable results. Fresh material showed very low reactivity with CH_4, and the reactivity increased with each reduction cycle, as is shown in Figure 8a. In Figure 8a, it can be seen that the iron oxide scales changed most rapidly during the early redox cycles. The particles appear to have become at least decently stable after a dozen cycles or so, and all data presented in this paper refers to particles that have passed this period.

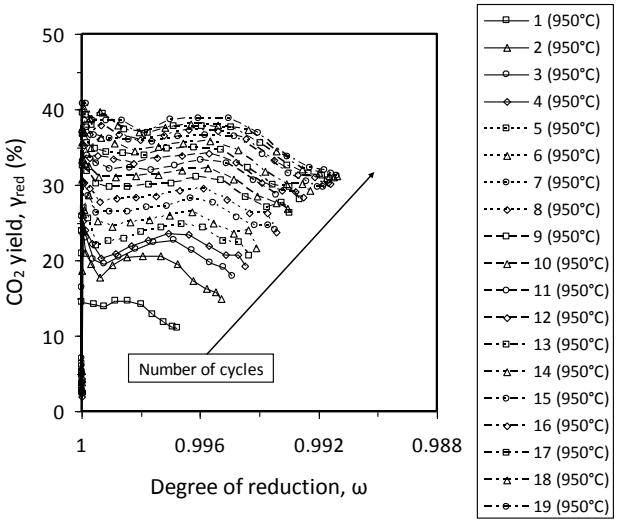

Figure 8a) γ_{red} as function of ω for iron oxide scales for 19 reduction cycles at 950°C, with F_{CH4}=0.45 L_n/min.

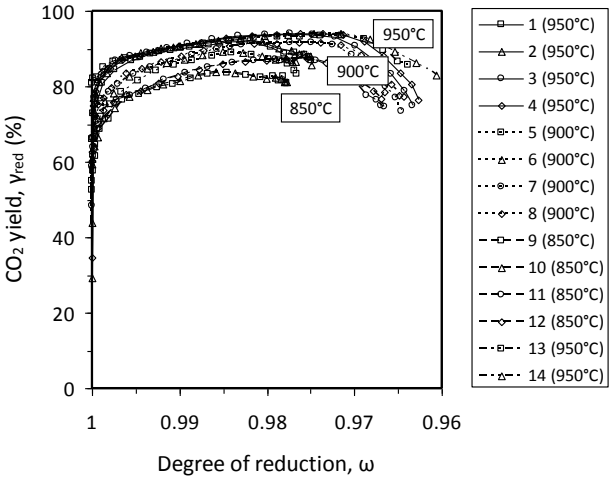

Figure 8b) γ_{red} as function of ω for iron oxide scales with 5 wt% N6AM400 for different reduction cycles and temperatures.

Used iron oxide scales were found to have 20-30% lower density compared to fresh material. Reduced density means higher porosity and increased active surface area, which could explain the improved reactivity. In Figure 7a, it can be seen that the used iron oxide scales appears to have swollen into a somewhat larger size. Further, the sharp edges and surface of the fresh particles have become smoother. A close look at the particle surface reveals cracks and grains, which likely contributes to an increase in the active surface area and reactivity.

In Figure 8b, γ_{red} as function of ω is shown for reduction of iron oxide scales with 5 wt% N6AM400, at a few temperatures. In general, the results appear to be comparable to or better than those obtained with red iron oxide, see Figure 5b. These results are more stable compared to those presented in Figure 5a, likely since they were performed using particles that already had experienced a large number of reductions and oxidations. Despite this, there were still tendencies towards improved conversion of CH_4 as function of cycle number though, which makes interpretation of the results obtained with addition of N6AM1400 somewhat tricky.

5. Discussion

All three examined materials contain roughly 99 wt% Fe_2O_3 as active phase. Despite this, they displayed significant differences in reduction behaviour and durability. So while it is clear that various waste materials from the steel industry could be useful as oxygen carriers for chemical-looping combustion, it is also clear that a better understanding of how factors such as impurities, geometry and porosity affect the properties of an oxygen carrier is needed. This will have to be examined in the future.

It is not trivial to predict how the examined oxygen-carrier particles would do in a continuously operating reactor, where they likely would have to last for thousands of reductions and oxidations at considerably higher gas velocities compared to the experiments presented here. It seems unlikely that the examined brown iron oxide particles would have survived for many hours in such conditions. But red iron oxide was fairly stable and could be a candidate for further work.

Iron oxide scales could also be an attractive oxygen carrier. Iron oxide scales experienced increasing reactivity and porosity during the experiments, but unlike brown iron oxide they did not show tendencies to break apart and form fines. The effect of adding N6AM1400 to iron oxide scales was larger compared to red iron oxide. Further, the cost for such particles should be extremely low. Iron oxide scales in the form used here is produced as by-product in ordinary steel mills and currently have no economic value. They could be used directly, and no additional manufacturing process should be needed.

6. Conclusion

The experiments presented in this paper show that waste materials from the steel industry could possibly be used as oxygen carrier for chemical-looping combustion applications. Fe_2O_3-containing waste materials react decently with CH_4 on their own, and addition of a 5 wt% N6AM1400 particles resulted in significantly more CO_2 being produced during the standard reduction procedures. Addition of 5 wt% Ni-olivine also improved the CO_2 yield somewhat, but not with as much as synthetic NiO particles.

Freeze granulated particles of red and brown iron oxide were found to have similar physical properties, but showed different reduction behaviour, with brown iron oxide producing several times as much CO as red iron oxide. Brown iron oxide also experienced severe erosion during reduction and oxidation. There is no obvious reason for the difference, except that brown iron oxide contained traces of Ca and Ti, in addition to impurities also present in red iron oxide.

Iron oxide scales had very different physical properties compared to the freeze-granulated particles, being heavier and less spherical. The reactivity of fresh iron oxide scales towards CH_4

was low, but increasing as function of the number of reduction cycles. The effect of adding NiO-material to iron oxide scales was even larger than for freeze-granulated particles, but the interpretation of these experiments is more uncertain due to the constantly improving reactivity of these particles. Iron oxide scales could be an interesting candidate for further work due to the very low cost of this material.

7. Acknowledgments

The authors wish to thank our financers, supporters and co-workers within the CACHET project, contract 019972 under the 6th framework program funded by the European Commission. We also wish to thank SSAB, who provided us with the examined oxygen-carrier materials.

8. References

Abad, A., Mattisson, T., Lyngfelt, A., Rydén, M., 2006. Chemical-looping combustion in a 300 W continuously operating reactor system using a manganese-based oxygen carrier. Fuel, 85, 1174-1185.

Abad, A., Mattisson, T., Lyngfelt, A., Johansson, M., 2007a. The use of iron oxide as oxygen carrier in a chemical-looping reactor. Fuel, 86, 1021-1035.

Abad, A., García-Labiano, F., de Diego, L., Gayán, P., Adánez, J., 2007b. Reduction kinetics of Cu-, Ni-, and fe-based oxygen carriers using syngas (CO + H2) for chemical-looping combustion. Energy & Fuels, 21, 1843-1853.

Abad, A., Adánez, J., García-Labiano, F., de Diego, L., Gayán, P., Celaya, J., 2007c. Mapping of the range of operational conditions for Cu-, Fe-, and Ni-based oxygen carriers in chemical-looping combustion. Chemical Engineering Science, 62, 533-549.

Adánez, J., De Diego, L. F., García-Labiano, F., Gayán, P., Abad, A., 2003a. Selection of oxygen carriers for chemical-looping combustion. Energy & Fuels, 18, 371-377.

Adánez, J., Gayán, P., Celaya, J., De Diego, L. F., García-Labiano, F., Abad, A., 2003b. Chemical Looping Combustion in a 10 kWth Prototype Using a Cu/OAl_2O_3 Oxygen Carrier: Effect of Operating Conditions on Methane Combustion. Industrial & Engineering Chemistry Research, 45, 6075-6080.

Adanez, J., Garcia-Labiano, F., de Diego, L. F., Gayan, P., Celaya, J., Abad, A., 2006. Nickel-Copper Oxygen Carriers To Reach Zero CO and H_2 Emissions in Chemical-Looping Combustion. Industrial & Engineering Chemistry Research**,** 45, 2617-2625.

Berguerand, N., Lyngfelt, A, 2008a. Design and Operation of a 10 kWth Chemical-Looping Combustor for Solid Fuels – Testing with South African Coal. Fuel, 87, 2713-2726.

Berguerand, N., Lyngfelt, A, 2008b. The Use of Petroleum Coke as Fuel in a 10 kWth Chemical-Looping Combustor. International Journal of Greenhouse Gas Control, 2, 169-179.

Brandvoll, Ø., 2005. Chemical looping combustion: fuel conversion with inherent CO_2 capture. Doctoral thesis, Norwegian University of Science and Technology, Trondheim, Norway.

Cho, P., 2005a. Development and characterization of oxygen-carrier materials for chemical-looping combustion. Doctoral thesis, Chalmers University of Technology, Göteborg, Sweden.

Cho, P., Mattisson, T., Lyngfelt, A., 2005b. Carbon formation on nickel and iron oxide-containing oxygen carriers for chemical-looping combustion. Industrial & Engineering Chemistry Research, 44, 668-676.

de Diego, L., García-Labiano, F., Gayán, P., Adánez, J., Celaya, J., Palacios, J. M., 2007. Operation of a 10 kWth chemical-looping combustor during 200 h with a $CuO–Al_2O_3$ oxygen carrier. Fuel, 86, 1036-1045.

García-Labiano, F., de Diego, L., Gayán, P., Adánez, J., Abad, A., 2006. Effect of pressure on the behavior of copper-, iron-, and nickel-based oxygen carriers for chemical-looping combustion. Energy & Fuels, 20, 26-33.

Jerndal, E., Mattisson, T., Lyngfelt, A., 2006. Thermal Analysis of Chemical-Looping Combustion. Chemical Engineering Research and Design, 84, 795-806.

Jin, H., Okamoto, T., Ishida, M., 1998. Development of a novel chemical-looping combustion: Synthesis of a looping material with a double metal oxide of CoO-NiO. Energy & Fuels**,** 12, 1272-1277.

Johansson, E., 2005. Fluidized-bed reactor systems for chemical-looping combustion with inherent CO_2 capture. Doctoral thesis, Chalmers University of Technology, Göteborg, Sweden.

Johansson, E., Mattisson, T., Lyngfelt, A., Thunman, H., 2006a. Combustion of syngas and natural gas in a 300 W chemical-looping combustor. Chemical Engineering Research and Design, 84, 819-827.

Johansson, E., Mattisson, T., Lyngfelt, A., Thunman, H., 2006b. A 300 W laboratory reactor system for chemical-looping combustion with particle circulation. Fuel, 85, 1428-1238.

Johansson, M., Mattisson, T., Lyngfelt, A., 2004. Investigation of Fe2O3 with $MgAl_2O_4$ for chemical-looping combustion. Industrial & Engineering Chemistry Research, 43, 6978-6987.

Johansson, M., Mattisson, T., Lyngfelt, A., 2006. Creating a synergy effect by using mixed oxides of iron- and nickel oxides in the combustion of methane in a chemical-looping combustion reactor. Energy & Fuels, 20, 2399-2407.

Johansson, M., 2007. Screening of oxygen-carrier particles based on iron-, manganese-, copper- and nickel oxides for use in chemical-looping technologies. Doctoral thesis, Chalmers University of Technology, Göteborg, Sweden.

Kolbitsch, P., Pröll, T., Bohlar-Nordenkampf, J., Hofbauer, H, 2008. Operating experience with chemical looping combustion in a 120kW dual circulating fluidized bed (DCFB) unit. Proceedings of the 9th International Conference on Greenhouse Gas Control Technologies, Washington, United States.

Kronberger, B., 2005. Modelling analysis of fluidised bed reactor systems for chemical-looping combustion. Doctoral thesis, Vienna University of Technology, Vienna, Austria.

Leion, H., 2008a. Capture of CO_2 from solid fuels using chemical-looping combustion and chemical-looping oxygen uncoupling. Doctoral thesis, Chalmers University of Technology: Göteborg, Sweden.

Leion, H., Lyngfelt, A., Johansson, M., Jerndal, E., Mattisson, T, 2008b. The use of ilmenite as an oxygen carrier in chemical-looping combustion. Chemical Engineering Research and Design, 86, 1017-1026.

Leion, H., Jerndal, E., Steenari, B. M., Hermansson, M., Israelsson, E., Jansson, M., Johnsson, R., Thunberg, A., Vadenbo, T., Lyngfelt, A., Mattisson, T., 2009a. Solid fuels in chemical-looping combustion using iron ore and oxide shells as oxygen carrier. Fuel, in press.

Leion, H., Lyngfelt, A., Mattisson, T, 2009b. The use of ores and industrial products as oxygen carrier in chemical-looping combustion. Energy & Fuels, in press.

Linderholm, C., Abad, A., Mattisson, T., Lyngfelt, A., 2008. 160 hours of chemical-looping combustion in a 10 kW reactor system with a NiO-based oxygen carrier. International Journal of Greenhouse Gas Control, 2, 520-530.

Linderholm, C., Jerndal, E., Mattisson, T., Lyngfelt, A., 2009a. Investigation of Ni-based mixed oxides in a 300-W chemical-looping combustor. Submitted for publication.

Linderholm, C., Mattisson, T., Lyngfelt, A., 2009b. Long-term integrity testing of spray-dried particles in a 10-kW chemical-looping combustor using natural gas as fuel. Fuel, in press.

Lyngfelt, A., Kronberger, B., Adánez, J., Morin, J.X., Hurst, P., 2004. The GRACE project. Development of oxygen carrier particles for chemical-looping combustion. Design and operation of a 10 kW chemical-looping combustor. Proceedings of the 7th International Conference on Greenhouse Gas Control Technologies, Vancouver, Canada.

Mattisson, T., Johansson, M., Lyngfelt, A., 2006. CO_2 capture from coal combustion using chemical-looping combustion – Reactivity investigation of Fe, Ni and Mn based oxygen carriers using syngas. Proceedings of the Clearwater Coal Conference, Clearwater, United States.

Mattisson, T., Johansson, M., Jerndal, E., Lyngfelt, A., 2008. The reaction of $NiO/NiAl_2O_4$ particles with alternating methane and oxygen. The Canadian Journal of Chemical Engineering, 86, 756-767.

Naqvi, R., 2006. Analysis of gas-fired power cycles with chemical looping combustion for CO_2 capture. Doctoral thesis, Norwegian University of Science and Technology, Trondheim, Norway.

Pröll, A., Mayer, M., Bohlar-Nordenkampf, J., Kolbitsch, P., Mattission, T., Lyngfelt, A., Hofbauer, H., 2008. Natural minerals as oxygen carriers for chemical-looping combustion in a dual circulating fluidized bed system. Proceedings of the 9th International Conference on Greenhouse Gas Control Technologies, Washington, United States.

Rydén, M., 2008a. Hydrogen production from fossil fuels with carbon dioxide capture, using chemical-looping technologies. Doctoral thesis, Chalmers University of Technology: Göteborg, Sweden.

Rydén, M., Lyngfelt, A., Mattisson, T, 2008b. Chemical-looping combustion and chemical-looping reforming in a circulating fluidized-bed reactor using Ni-based oxygen carriers. Energy & Fuels, 24, 2585-2597.

Ryu, H.J., Jin, G.T., Yi, C.K., 2004. Demonstration of inherent CO_2 separation and no NO_X emission in a 50 kW chemical-looping combustor - continuous reduction and oxidation experiment. Poster presented at the 7th International Conference on Greenhouse Gas Control Technologies, Vancouver, Canada.

Son, S. R., Kim, S. D., 2006. Chemical-Looping Combustion with NiO and Fe2O3 in a Thermobalance and Circulating Fluidized Bed Reactor with Double Loops. Industrial & Engineering Chemistry Research**,** 45, 2689-2696.

Wolf, J., 2004. CO_2 mitigation in advanced power cycles. Doctoral thesis, the Royal Institute of Technology, Stockholm, Sweden.

Zafar, Q., Abad, A., Mattisson, T., Gevert, B., 2007a. Reaction kinetics of freeze-granulated $NiO/MgAl_2O_4$ oxygen carrier particles for chemical-looping combustion. Energy & Fuels, 21, 610-618.

Zafar, Q., Abad, a., Mattisson, T., Gevert, B., Strand, M., 2007b. Reduction and Oxidation Kinetics of $Mn_3O_4/Mg\text{-}ZrO_2$ Oxygen Carrier Particles for Chemical-Looping Combustion. Chemical Engineering Science, 62, 6556-6567.